Composite Structures 135 (2016) 140–155

Analytical Solution for Bending of Laminated Composites with Matrix Cracks

Ever J. Barbero[1]
and
Javier Cabrera Barbero[2]

Abstract

An analytical, closed form solution is developed for balanced (not necessarily symmetric) laminates subjected to flexural deformation. The analytical solution provides spatial distribution of displacements and curvature, from which in-plane and intralaminar strains and stresses are obtained through differentiation and constitutive equations. The deformation is shown to consist of a homogeneous deformation plus perturbations near the crack tip. A methodology is proposed to separate the perturbation from the homogeneous deformation, to eliminate ill-conditioning of the eigenvalue/eigenvector problems that occurs otherwise. It is shown that, while the homogeneous deformation provides a macroscopic measure of damage in terms of reduced flexural stiffness of the laminate, the perturbation solution provides a detailed account of the intralaminar shear induced near the crack, which is used to calculate the extent of shear lag and the maximum intralaminar shear stress. The intact portion of the laminate is modeled without lumping it into a single equivalent lamina. Furthermore, laminas can be subdivided into multiple sub-laminates to increase the accuracy of the representation of intralaminar/interlaminar shear, which is shown to improve the predicted value of maximum interlaminar shear stress, which in turn is important for the prediction of matrix-crack induced delamination.

[1]Professor, West Virginia University, Morgantown, USA. Corresponding author.
[2]Undergraduate student, Universidad Carlos III de Madrid, Madrid, Spain.
The final publication is available at http://dx.doi.org/10.1016/j.compstruct.2015.09.021

Keywords

Matrix damage; Intralaminar damage; Perturbation solution; Shear lag; Bending stiffness; Homogeneous flexural deformation.

1 Introduction

Intralaminar matrix cracking is the first mode of damage in polymer-matrix laminated composites subjected to quasi-static, fatigue, and impact load. Matrix cracking increases the permeability of the laminate leading to gas/liquid leakage and facilitates access to contaminants that may degrade the fibers. Also, matrix cracking often precedes catastrophic modes of damage such as delamination, and fatigue life reduction. Furthermore, stiffness reduction of cracking laminas leads to stress redistribution to other laminas that may as a result fail in a catastrophic, fiber dominated mode. Therefore, prediction of damage initiation and evolution is an important ingredient of laminate failure prediction [1].

Matrix cracks are caused by a combination of transverse tensile and in-plane shear strain. Under these conditions, preexisting defects grow into cracks when the energy release rate exceeds the intralaminar fracture toughness of the lamina. Assuming linear elastic fracture mechanics [2] and periodicity leads to predictive methods that require the minimum number of material properties while achieving good comparisons with available experimental data. These solutions are either approximate, e.g., [3–7] or numerical, e.g., [8–11]. More refined methods require adjustable parameters, for example in the form of empirical hardening laws [12, 13], and combinations of fracture and strength properties, for example [14].

The vast majority of analytical and semi-analytical solutions are restricted to symmetric laminates subjected to membrane loads only, and only matrix cracks are considered for the calculation of interlaminar stresses. To account for interaction between intralaminar cracks and delaminations, more complex numerical models such as reported in [15] are needed. Furthermore, most analytical and semi-analytical solutions assume either linear [16] or bi-linear [17] distribution of interlaminar stress through the undamaged sublaminates. Such limitation is removed in this work by subdividing each undamaged lamina into a sublaminate with as many layers as needed to achieve convergence in the value of the maximum interlaminar stress.

Matrix cracking of laminates subject to flexural deformation are analyzed in [18, 19] using a clever analogy between laminates and orthotropic media. Such methodology was generalized in [20], but it relies on an "a priori" parametric study via finite element analysis (FEA) that restricts its applicability to those material systems included in the FEA study. A 1D beam bending model for $[0/90]_S$–like laminates where only one of the 90° laminas is allowed to crack is offered in [21, 22]. The finite strip solution in [23–25] relies on the generalized plane strain assumption.

Both approximate and numerical solutions require either experiments or analytical solutions to validate them. Experiments are limited to a few laminate configurations and they are further limited in what can be measured. For example, stiffness reduction of carbon fiber laminates is very difficult to measure. Therefore, analytical solutions are desirable because they can be used as benchmarks, even if they are limited in scope of applicability to say, plane stress, and/or impose restrictions on the type of material behavior, such as say, elastically linear/damaging behavior.

In this work, a *closed form, analytical* solution is developed for balanced (not necessarily symmetric) laminates subjected to bending. Plane stress through the thickness and along one of the in-plane directions is assumed to reduce the problem to one dimension. The analytical solution provides spatial distribution of displacements and curvature, from which in-plane and intralaminar strains are obtained through differentiation, and stresses through constitutive equations. The solution is expressed as a combination of a fundamental solution and perturbation functions to represent the perturbation of the stress/strain field near the cracks. In this way, the near singularity of displacement-only solutions is removed. Furthermore, the perturbation terms lead naturally to computation of intralaminar/interlaminar stresses.

2 Approximations

The development of a closed form, analytical solution for bending of laminates with matrix cracks requires a number of approximations to reduce the 3D problem to 1D. These approximations are described as follows.

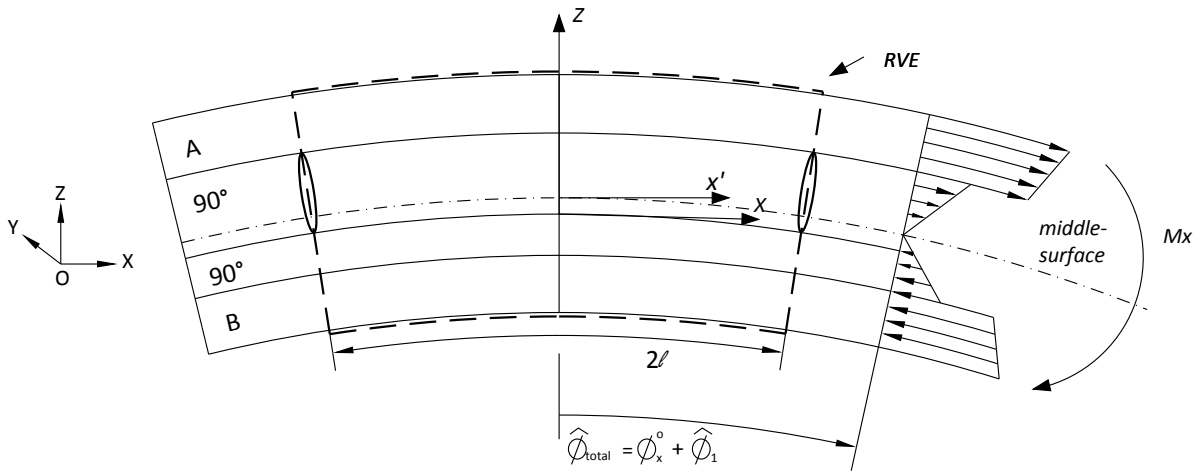

Figure 1: Representative Volume Element (RVE) with dimensions $2\ell \times 1 \times 2h$, where $2h$ is the thickness of the laminate, and A,B, represent balanced sub-laminates.

2.1 Fracture mechanics

Consider a thin, balanced laminate, with N laminas, subjected to bending load M_x only. All laminas are of the same material but oriented with respect to the x-axis in a laminate stacking sequence (LSS) such as $[0_m/90_n/\pm\theta_r]_S$, where $\theta < 45°$. Experimental evidence [26–33] indicate that in such laminates, the transverse laminas develop cracks as soon as the energy release rate in mode-I fracture G_I exceeds the intralaminar fracture toughness of the material G_{Ic}. Cracks start at defects within the transverse layer (90_n layer). Their propagation through the thickness of the ply is unstable [34, section 7.2.1], reaching the interface suddenly. Upon further increase in applied load M_x or curvature κ_x, the thickness cracks grow again unstably parallel to the fiber direction, as illustrated in Figure 1.

When subjected to bending deformation, only the laminas experiencing tensile stress may develop matrix cracks parallel to the fiber direction. If the cracked lamina spans across the midsurface, the thickness crack develops on the tensile side only. In this case, the transverse lamina is divided into two laminas, one cracked (tensile side) and another one virgin (compression side).

Initially, cracks are not equally spaced but they become so as the crack density increases [35]. It is therefore possible to assume equally spaced cracks, which allows us to assume periodicity, and thus identify and use a representative volume element (RVE) to analyze this problem efficiently. The RVE encompasses the thickness of the laminate, a unit length along the fiber direction of the

cracking lamina, and the arc length 2ℓ between existing cracks. The crack density in each lamina, denoted by subscript i, is defined as

$$\lambda_i = 1/2\ell \tag{1}$$

The analysis assumes that a very small crack density exists in the material, which may be justified as being representative of initial defects. An initial value $\lambda_i = 0.01\ mm^{-1}$ is used in the examples. New cracks are assumed to appear halfway between existing cracks, that is, as far as possible from the shear lag regions near existing cracks. The coordinate system for the RVE has its origin halfway between existing cracks, as shown in Figure 1.

2.2 Plate kinematics

In this work, general laminates, such as $[0_m/90_n/\pm\theta_r]$, not necessarily symmetric, can be analyzed. Even if the undamaged (intact) laminate is initially symmetric, it will become unsymmetric when it cracks on the tensile side of the midsurface. Furthermore, bending deformation is antisymmetric with respect to the midsurface, with positive (negative) deformation above (below) the midsurface. In summary, due to antisymmetry of deformation and material properties with respect to the mid-surface of the laminate, all the laminate (with N laminas) needs to be analyzed. The following approximations are made:

I. Lines initially straight and normal to the mid-surface remain incompressible: $\epsilon_z \simeq 0$

II. A state of plane stress is assumed in the thickness direction, i.e., $\sigma_z^i = 0$

III. Due to intralaminar damage, a high order kinematics is needed to represent the beam deformation, and consequently lines initially straight and normal to the mid-surface are no longer straight and normal to the mid-surface. Furthermore, the deflection w^0 and the rotation ϕ_x^0 are not zero. Since the laminate is balanced, the deformation is symmetric with respect to the $y-z$ plane (Fig. 1), and no bending is applied in the $y-$direction ($M_y = 0$), the intralaminar shear strain for each lamina can be written as the deviation from the average laminate rotation, as follows

$$\gamma_{xz}^{i} = \frac{\partial u^{i}}{\partial z} - \phi_{x}^{0} \tag{2}$$

where $u_i(x, z)$ is the in-plane displacement of the $i-$lamina.

IV. In order to reduce the problem to 2D, a state of plane stress is assumed in the $y-$direction, i.e., $\sigma_y^i = 0$.

V. For a general laminate such as $[0_m/90_n/\pm\theta_r]$, the coupling terms D_{16} and D_{26} may be different from zero, but these terms decrease rapidly with increasing r. Therefore, each pair $(\pm\theta)$ is treated as an equivalent lamina without coupling ($Q_{16} = Q_{26} = 0$) and therefore $D_{16} = D_{26} = 0$ and $\gamma_{xy}^i = 0$.

VI. Since cracks appear equally spaced on both sides of the $y - z$ plane (Figure 1), the domain is symmetric with respect to the $y - z$ plane and $\gamma_{yz}^i = 0$.

The sum of approximations I to VI reduce the problem to 2D, i.e.,

$$\begin{cases} u^{i} = u^{i}(x,z) = z\,\phi_{x}^{o}(x) + u_{1}^{i}(x,z) \\ w^{i} = w^{o}(x) \end{cases} \tag{3}$$

where $\phi_x^o(x)$ is the fundamental solution and $u_1^i(x, z)$ are perturbations produced by intralaminar cracks. The strain field in each lamina of the laminate can be written as follows

$$\begin{Bmatrix} \epsilon_x \\ \epsilon_y \\ \gamma_{xy} \end{Bmatrix}^{i} = z \begin{Bmatrix} \partial\phi_x^o/\partial x \\ 0 \\ 0 \end{Bmatrix} + \begin{Bmatrix} \partial u_1^i(x,z)/\partial x \\ 0 \\ 0 \end{Bmatrix} \tag{4}$$

and the Poisson's effect $\epsilon_y^i \approx 0$ is assumed to be negligible.

3 Constitutive equations

Let's denote by subscript k the particular lamina that is, at the moment, subject to cracking, which in this study will be one of the laminas oriented at 90 degrees with respect to the x-axis, subjected

to tensile stress, taken one at a time. Let's denote with subscript $m \neq k$ all other laminas that are not cracking at the moment, which are $N-1$ of them. If more than one cracking lamina exist, they will be analyzed one at a time. For a state of plane stress we have

$$\begin{Bmatrix} \epsilon_x \\ \epsilon_y \\ \gamma_{xy}=0 \end{Bmatrix}^i = \begin{bmatrix} \bar{S}_{11} & \bar{S}_{12} & \bar{S}_{16} \\ \bar{S}_{12} & \bar{S}_{22} & \bar{S}_{26} \\ \bar{S}_{16} & \bar{S}_{26} & \bar{S}_{66} \end{bmatrix}^i \begin{Bmatrix} \sigma_x \\ \sigma_y=0 \\ \sigma_{xy} \end{Bmatrix}^i ; \quad \begin{Bmatrix} \gamma_{yz}=0 \\ \gamma_{xz} \end{Bmatrix}^i = \begin{bmatrix} \bar{S}_{44} & \bar{S}_{45} \\ \bar{S}_{45} & \bar{S}_{55} \end{bmatrix}^i \begin{Bmatrix} \tau_{yz} \\ \tau_{xz} \end{Bmatrix}^i \tag{5}$$

Note that each balanced pair $\pm\theta$ is treated as a single lamina with $\bar{S}_{16} = \bar{S}_{26} = \bar{S}_{45} = 0$. Therefore, the problem has symmetry with respect to the y-z plane, and as a result $\tau^i_{yz} = 0$. Using these facts, as well as (2) in (5), we get

$$\frac{\partial u^i(x,z)}{\partial z} - \phi^o_x = \bar{S}^i_{55}\, \tau^i_{xz} \tag{6}$$

The constitutive equation of lamina i, expressed in lamina coordinate system (c.s. 1,2,3) is

$$\sigma^i_r = \left[Q^i_{rs}\right] (\epsilon^i_s - \alpha^i_s \Delta T); \quad r,s = 1,2,6 \tag{7}$$

where α is the coefficient of thermal expansion (CTE), ΔT is the increment of temperature, and $[Q^i_{rs}]$ is the stiffness matrix of the lamina, possibly reduced due to prior damage, and expressed in the lamina c.s. Once the crack density λ_k in lamina k is known, and the reduced stiffness of the laminate $[Q(\lambda)]$ has been calculated, the reduced stiffness matrix $[Q^k(\lambda)]$ of lamina k is calculated as

$$[Q^k]\, h^k = [Q(\lambda)]\, h - \sum_{m=1}^{N} (1-\delta_{mk})[Q^m]\, h_m \tag{8}$$

where δ is the Kronecker symbol and $h = \sum_{i=1}^{N} h_i$ is the thickness of the laminate. To aid in computer implementation, the following damage variables are defined

$$D_{ij}^k(\lambda_k) = 1 - Q_{ij}^k/\widetilde{Q}_{ij}^k; \quad i = 1,2,6\ ;\ j = 2,6 \tag{9}$$

where $\widetilde{Q}_{ij}^k$ is the virgin stiffness matrix of the lamina. In this way, the reduced stiffness of any damaged lamina can be easily calculated as

$$\left[Q^k\right] = \begin{bmatrix} \widetilde{Q}_{11}^k & (1-D_{12})\widetilde{Q}_{12}^k & 0 \\ (1-D_{12})\widetilde{Q}_{12}^k & (1-D_{22})\widetilde{Q}_{22}^k & 0 \\ 0 & 0 & (1-D_{66})\widetilde{Q}_{66}^k \end{bmatrix} \tag{10}$$

Based on experimental evidence [28–31], laminas at 0°, transverse laminas subjected to compression stress, and groups $\pm\theta < 45°$, all of which are denoted by subscript m, are assumed to be free from cracking when the laminate is loaded with M_x only. Laminas at 90° with tensile stress, denoted by subscript k, are assumed to crack when the energy release rate in fracture mode I, G_I, reaches the intralaminar fracture toughness G_{Ic}.

Although the intact laminate is symmetric, the damaged laminate is unsymmetric. Therefore, bending-extension coupling terms β_{ij} appear when using the original coordinate system. Since the laminate is balanced (assumption V), the constitutive equations of the cracked laminate can be simplified as follows [34, Sect. 10.2.1]

$$\begin{Bmatrix} \epsilon_x^o \\ \epsilon_y^o \\ \gamma_{xy}^o \\ \kappa_x \\ \kappa_y \\ \kappa_{xy} \end{Bmatrix} = \begin{bmatrix} \alpha_{11} & \alpha_{12} & 0 & \beta_{11} & \beta_{12} & 0 \\ & \alpha_{22} & 0 & \beta_{12} & \beta_{22} & 0 \\ & & \alpha_{66} & 0 & 0 & \beta_{66} \\ & & & \delta_{11} & \delta_{12} & 0 \\ & & & & \delta_{22} & 0 \\ sym. & & & & & \delta_{66} \end{bmatrix} \begin{Bmatrix} N_x \\ N_y = 0 \\ N_{xy} \\ M_x \\ M_y = 0 \\ M_{xy} \end{Bmatrix} \tag{11}$$

where N_x, N_y and N_{xy} are the normal and shear forces per unit length on the sides with units [N/m]; M_x, M_y and M_{xy} are the moments per unit length on the sides, with units [N], with bending moments taken as are positive when they produce a concave deformation looking from the negative z-axis (Fig. 1); $\epsilon_x^o, \epsilon_y^o$, and ϵ_{xy}^o are the mid-plane strains, and κ_x, κ_y, and κ_{xy} the curvatures.

The compliance matrix in (11) is the inverse of the ABD matrix [34, Eq. (6.16)], with the lamina reduced stiffness $[Q]^k$ calculated for the current crack density λ using (10) as in [36]. In this way, the compliance in (11) contains bending-extension coupling even if the intact laminate was symmetric before it cracked. Once cracked, the laminate is no longer symmetric.

Removing the first and fifth rows and columns from (11), inverting and reorganizing terms, the constitutive equation for the laminated beam becomes (see [34, Ch. 10])

$$\begin{Bmatrix} \epsilon_x \\ \kappa_y \\ \gamma_{xy} \\ \kappa_x y \end{Bmatrix} = \begin{bmatrix} A & B & 0 & 0 \\ B & D & 0 & 0 \\ 0 & 0 & F & C \\ 0 & 0 & C & H \end{bmatrix} \begin{Bmatrix} N_x \\ M_x \\ N_{xy} \\ M_{xy} \end{Bmatrix} \tag{12}$$

where A, B, C, D, F, H, are scalars representing the various stiffnesses of the laminated beam; A is the axial stiffness, B represents the coupling between bending and extension, D is the bending stiffness, H is the twisting stiffness, F is the in-plane shear stiffness, and C is the coupling between twisting curvature and in-plane shear. The position of the neutral axis of bending is given by

$$e_b = \frac{B}{A} \tag{13}$$

The eccentricity e_b displaces the original coordinate system, uncoupling the bending and extensional forces, and allowing us to obtain a new mid-surface for which $B = 0$ (Figure 1). Once the position of the neutral axis (13) is known, the new z coordinates of all interfaces can be calculated by subtracting e_b from the original z coordinates of the interfaces between laminas. If a cracking lamina straddles the midsurface of the laminate, that lamina will now be divided in two laminas of different thicknesses so that the crack extends to the neutral axis.

Developing and simplifying (7) along the x-direction, we get

$$\sigma_x = E_x^i(\epsilon_x^i - \alpha_x^i \Delta T) \tag{14}$$

where α^i and E_x^i are the coefficient of thermal expansion and the modulus of elasticity of the $i-$lamina in the laminate coordinate system x,y, respectively, with

$$E_x^i = \bar{Q}_{11}^i - \frac{(\bar{Q}_{12}^i)^2}{\bar{Q}_{22}^i} \tag{15}$$

where $\bar{Q}_{ij}^i$ are the stiffnesses of lamina i transformed to the laminate c.s. (i.e., x,y). Substituting ϵ_x^i from (4) into (14), we get

$$\sigma_x = E_x^i \left(z_i \frac{\partial \phi_x^o(x)}{\partial x} + \frac{\partial u_1^i(x,z)}{\partial x} - \alpha_x^i \Delta T \right) \tag{16}$$

4 Deformation

The moment-curvature equation for a laminated beam is

$$\kappa_x^0 = \frac{M_x}{(EI)} = \delta_{11} M_x = \frac{\partial \phi_x^0}{\partial x} \tag{17}$$

where the last term is the rotation-curvature relationship from first order shear deformation theory (FSDT) [34, Ch. 6], the superscript ^{o} indicates *laminate* quantities that are independent of z, (EI) is the bending stiffness [34, Ch. 10], and $\delta_{11} = (EI)^{-1}$ is the bending compliance given by

$$\delta_{11} = \left[\frac{D_{11} D_{22} - D_{12}^2}{D_{22}} \right]^{-1} \tag{18}$$

in terms of the bending stiffness matrix $[D]$ of the intact laminate. In this way, κ_x^o is the curvature of the FSDT fundamental solution, which will be complemented with the perturbation solution due to cracking, later on.

The axial deformation $u(x)$ can obtained from the FSDT kinematics (flexure only) as follows

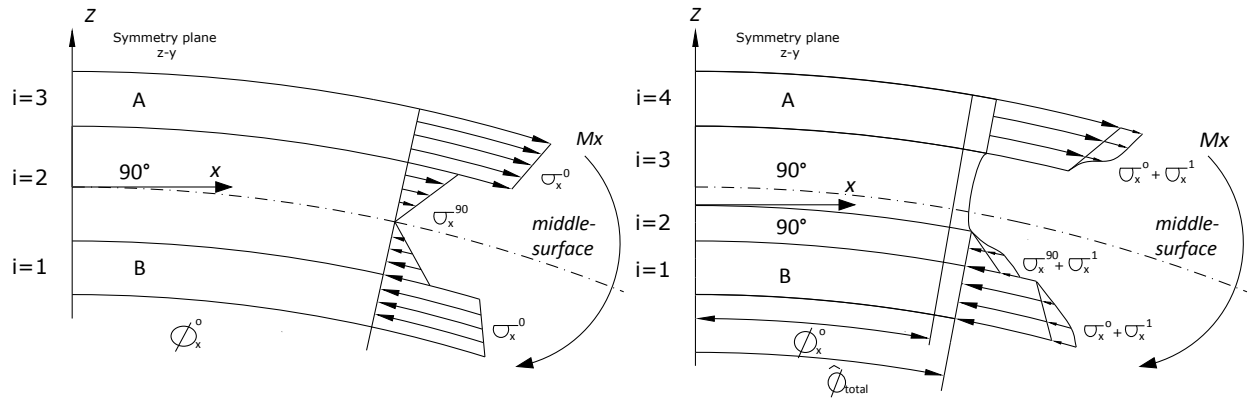

Figure 2: Through-the-thickness distribution of normal stress (a) before and (b) after the crack. The cracked lamina is numbered $k = 3$ with fiber orientation $\theta = 90°$.

$$u(x, z) = z\ \phi_x^0(x) \tag{19}$$

Therefore, the strain is linear through the thickness

$$\epsilon_x(x, z) = z\ \frac{\partial \phi_x^0}{\partial x} \tag{20}$$

and the stress is piecewise linear through the thickness, as shown in Figure 2(a) (due to the different stiffnesses of the laminas).

For the undamaged laminate, no interlaminar shear is necessary to satisfy continuity of displacements through the thickness. If a crack appears in lamina k, the surface of the crack becomes a free edge, unable to support stress. To maintain equilibrium, the stress in the rest of laminas must increase, as depicted in Figure 2(b). The resulting stress distribution is unknown and not necessarily piecewise linear, but the summation of all the stress *perturbations* in the uncracked laminas must compensate for loss of the stress in the cracked lamina ($k = 3$ counting from the bottom in Figure 2). In other words, the stress no longer carried by the cracked lamina must be taken up by the remaining uncracked laminas. The laminate becomes unsymmetric, requiring us to study the entire the laminate, as well as its eccentricity, even if initially symmetric.

To helps us understand the proposed kinematics, let's consider (as an example and without

loss of generality) the case of symmetric *laminate stacking sequence* (LSS) subjected to flexural deformation only. When such laminate is intact, the displacement distribution $u(z)$ is antisymmetric (i.e., a linear function of z in (19)). When such laminate becomes cracked, the displacement distribution should remain, for the most part, approximately antisymmetric.

Since the axial stress σ_x vanishes at the crack surface, interlaminar stresses τ_{xz} are necessary to satisfy continuity of displacements at the interface between the cracked and adjacent laminas. The interlaminar stress τ_{xz} is zero at the top and bottom of the laminate because those are free surfaces.

Furthermore, both of the interfaces limiting the cracked lamina are *subjected to* intralaminar stress of the same direction (Figure 3), in this case to the right, in order to equilibrate the tensile stress on the left of the 90 lamina (k=3) with a crack on the right. The opposite signs (positive on the top face of k=3, and negative on bottom) are due to the opposite sign of the normal at the two interfaces (positive on top and negative on bottom). Note that the arrows show the intralaminar stress *applied to* the lamina *by* the adjacent laminas.

Continuity of intralaminar strain $\gamma_{xz}(z)$ inside the cracked lamina demands that the intralaminar stress vanishes at one point within the cracked lamina, as shown on the right hand side of Figure 3, but not necessarily at the midsurface of the cracked lamina because of the influence of the flexural deformation.

Since the fundamental solution for the displacements (19) (before the crack appears) is antisymmetric, the total displacement distribution $u(z)$ (after the crack appears) should be almost antisymmetric. Also note that the interlaminar stress is proportional to the change in displacement along z, i.e., $\tau_{xz} \propto \partial u/\partial z$, and an antisymmetric displacement distribution satisfies $\partial u/\partial z > 0$. Therefore, the interlaminar stresses in most if not all of the uncracked laminas will tend to be positive. Therefore, its distribution through the thickness must be an odd function. The simplest odd function is a linear distribution, as shown in Figure 3.

A linear distribution of shear stress in a lamina requires displacements $u^i(z)$ that are not linear in z, and for the cracked lamina they must be almost antisymmetric with respect to the lamina centerline, thus approximately quadratic in z. Since the solution of the equations of elasticity for such a problem is intractable, additional approximations are introduced, which reduce the problem to 1D, but still allows us to obtain an accurate representation for intralaminar/interlaminar stresses.

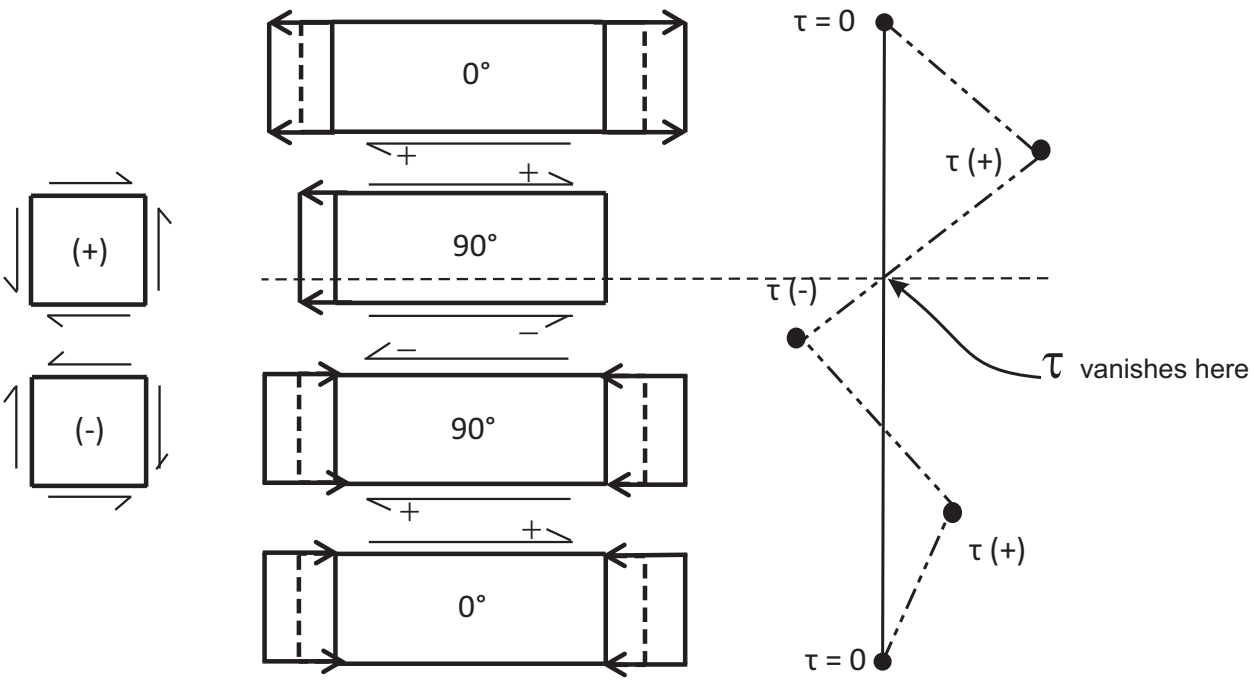

Figure 3: Layerwise linear distribution of intralaminar stress for a $[0/90]_S$ laminate. The full laminate is shown. The cracked lamina is numbered $k = 3$ with fiber orientation $\theta = 90°$.

Let's introduce the following averaging functions

$$\widehat{f} = \frac{1}{h_i} \int_{h_i} f(z)\, dz \tag{21}$$

$$\widehat{f}' = \frac{1}{h_i} \int_{z^{i-1,i}}^{z^{i,i+1}} f(z^{i-1,i} - z)\, dz \tag{22}$$

Equation (21) provides the average of any function f over the thickness of a lamina. When f is the displacement $u^i(x, z)$ of the $i-$lamina, equation (21) provides the average displacement $\widehat{u}(i)$ of the $i-$lamina. Equation (22) provides the displacement of a lamina relative to the top interface, the later denoted as the "$i, i+1$" interface, where i is the lamina number stating with $i = 1$ at the bottom of the laminate.

Let's consider the generic laminate displayed in Figure 4 and the coordinate system shown in Figure 5. The interlaminar stress is assumed to be linear, as follows

$$\tau_{xz}^i(x, z) = \tau_{xz}^{i,i+1}(x) + \left[\tau_{xz}^{i-1,i}(x) - \tau_{xz}^{i,i+1}(x)\right] \frac{z^{i,i+1} - z}{h_i} \tag{23}$$

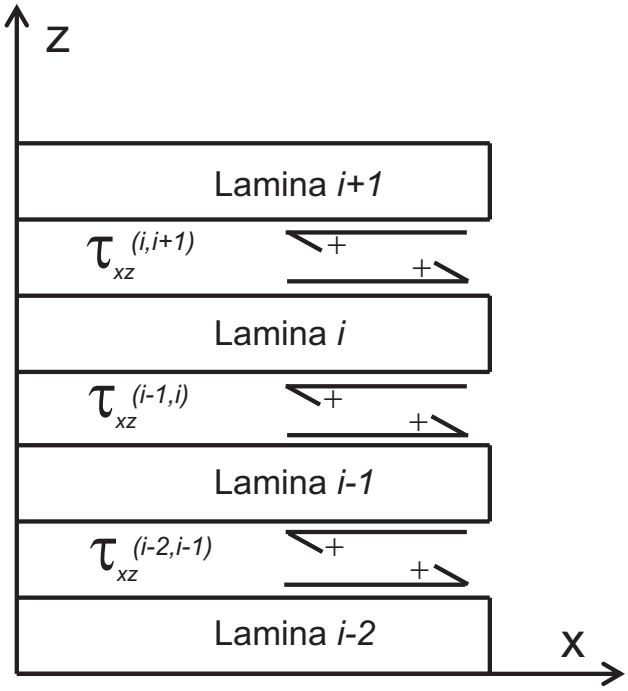

Figure 4: Generic laminate illustrating the numbering of laminas and interface shear stresses.

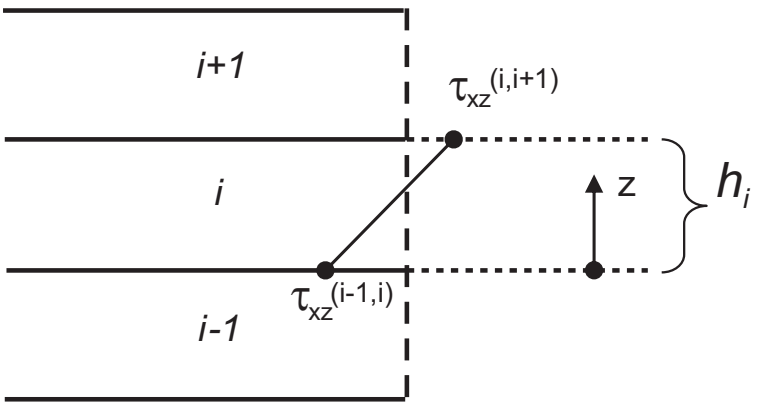

Figure 5: Local coordinate system at lamina i.

Note that assuming intralaminar stress τ_{xz}^{i} to be linear through the thickness implies a quadratic displacement $u^{i}(x,z)$ through the thickness, where the quadratic part must be confined to the second term in (3) because the first term is obviously linear in z. Therefore, equation (3) describes the kinematics of the laminate with a piece-wise quadratic deformation that satisfies zero interlaminar stress on the surfaces of the laminate as depicted in Figure 3. Calculating the weighted average (22) of (6) with τ_{xz}^{i} given by (23), we get

$$\begin{aligned}&\frac{1}{h_i}\int_{z^{i-1,i}}^{z^{i,i+1}}\frac{\partial u^i}{\partial z}(z^{i,i+1}-z)dz=\\&\frac{1}{h_i}\,\bar{S}_{55}^{i}\int_{z^{i-1,i}}^{z^{i,i+1}}\tau_{xz}^{i,i+1}\,(z^{i,i+1}-z)\,dz+\frac{1}{h_i}\,\bar{S}_{55}^{i}\int_{z^{i-1,i}}^{z^{i,i+1}}\left[\tau_{xz}^{i-1,i}-\tau_{xz}^{i,i+1}\right]\frac{(z^{i,i+1}-z)^2}{h_i}\,dz+\\&\frac{1}{h_i}\int_{z^{i-1,i}}^{z^{i,i+1}}\phi_x^{o}\,(z^{i,i+1}-z)\,dz\end{aligned}\tag{24}$$

Developing the LHS of (24) we get

$$\frac{1}{h_i}\left[\int_{z^{i-1,i}}^{z^{i,i+1}}\frac{\partial u^i}{\partial z}z^{i,i+1}dz-\int_{z^{i-1,i}}^{z^{i,i+1}}\frac{\partial u^i}{\partial z}zdz\right]\tag{25}$$

Integrating we get

$$\frac{1}{h_i}\,\left[\,z^{i,i+1}\,u^i(z^{i,i+1})\,-\,z^{i,i+1}\,u^i(z^{i-1,i})\,+\,z^{i-1,i}\,u^i(z^{i-1,i})\,-\,z^{i,i+1}\,u^i(z^{i,i+1})\right]+\frac{1}{h_i}\,\int_{z^{i-1,i}}^{z^{i,i+1}}u^i\,dz\tag{26}$$

and simplifying we have

$$\frac{1}{h_i}\,\left[\,z^{i-1,i}\,-\,z^{i,i+1}\,\right]\,u^i(z^{i-1,i})\,+\,\widehat{u}(i)\tag{27}$$

where $\widehat{u}(i)$ is the average displacement in the $i-$lamina according to (21). In this way, the problem is reduced from 2D to 1D, where the unknown variables $\widehat{u}(i)$ are only function of x. Therefore, (27)

reduces to

$$\widehat{u}(i) - u(z^{i-1,i}) \tag{28}$$

which we realize is equal to $\partial u^i/\partial z$. Integrating the first term on the RHS of (24) we have

$$-\frac{\bar{S}^i_{55}}{h_i}\tau^{i,i+1}_{xz}\left[\frac{(z^{i,i+1}-z)^2}{2}\right]^{z^{i,i+1}}_{z^{i-1,i}} = \bar{S}^i_{55}\frac{h_i}{2}\tau^{i,i+1}_{xz} \tag{29}$$

Integrating the second term on the RHS of (24) we have

$$-\frac{\bar{S}^i_{55}}{h_i}\frac{\left[\tau^{i-1,i}_{xz}-\tau^{i,i+1}_{xz}\right]}{h_i}\left[\frac{(z^{i,i+1}-z)^3}{3}\right]^{z^{i,i+1}}_{z^{i-1,i}} = \bar{S}^i_{55}\frac{h_i}{3}\left[\tau^{i-1,i}_{xz}-\tau^{i,i+1}_{xz}\right] \tag{30}$$

Integrating the third term on the RHS of (24) we have

$$-\frac{1}{h_i}\phi^o_x\left[\frac{(z^{i,i+1}-z)^2}{2}\right]^{z^{i,i+1}}_{z^{i-1,i}} = \frac{h_i}{2}\phi^o_x \tag{31}$$

Substituting (28),(29),(30),(31) into (24), we get

$$\widehat{u}(i) - u(z^{i-1,i}) = \bar{S}^i_{55}\frac{h_i}{2}\tau^{i,i+1}_{xz} + \bar{S}^i_{55}\frac{h_i}{3}\left[\tau^{i-1,i}_{xz}-\tau^{i,i+1}_{xz}\right] + \frac{h_i}{2}\phi^o_x \tag{32}$$

Next, let's consider the coordinate system shown in Figure 6. The interlaminar stress is again assumed to be linear, as follows

$$\tau^{i-1}_{xz}(x,z) \;=\; \tau^{i-2,i-1}_{xz}(x) \;+\; \left[\tau^{i-1,i}_{xz}(x) - \tau^{i-2,i-1}_{xz}(x)\right]\frac{z - z^{i-2,i-1}}{h_{i-1}} \tag{33}$$

Calculating the weighted average (22) of (6) with τ^i_{xz} given by (33), and following the same procedure that led to (32), we get

$$u(z^{i-1,i}) - \widehat{u}(i-1) = \bar{S}^{i-1}_{55}\frac{h_{i-1}}{2}\tau^{i-1,i-2}_{xz} + \bar{S}^{i-1}_{55}\frac{h_{i-1}}{3}\left[\tau^{i-1,i}_{xz}-\tau^{i-2,i-1}_{xz}\right] + \frac{h_{i-1}}{2}\phi^o_x \tag{34}$$

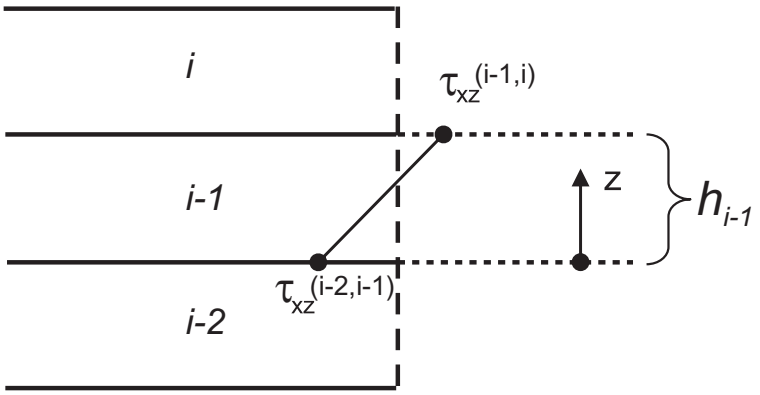

Figure 6: Local coordinate system at lamina *i-1*.

Adding (34) and (32) we get

$$\widehat{u}(i)-\widehat{u}(i-1)=\tau_{xz}^{i,i+1}\bar{S}_{55}^{i}\frac{h_i}{6}+\tau_{xz}^{i-1,i}\left[\bar{S}_{55}^{i}\frac{h_i}{3}+\bar{S}_{55}^{i-1}\frac{h_{i-1}}{3}\right]+\tau_{xz}^{i-2,i-1}\bar{S}_{55}^{i-1}\frac{h_{i-1}}{6}+\frac{1}{2}[h_i+h_{i-1}]\phi_x^o \quad (35)$$

Equation (35) provides the step change in average displacement from one lamina to the next in terms of the intralaminar shear values. But actually what is needed is the inverse, i.e., and equation for the intralaminar shear in terms of displacements. To obtain such relationship, we write (35) for the $N-1$ interfaces, as follows

$$-[H_o]\frac{\phi_x^o}{2}+\begin{Bmatrix}\widehat{u}(2)-\widehat{u}(1)\\ \widehat{u}(3)-\widehat{u}(2)\\ \vdots\\ \widehat{u}(N)-\widehat{u}(N-1)\end{Bmatrix}=[H]\begin{Bmatrix}\tau_{xz}^{1,2}\\ \tau_{xz}^{2,3}\\ \vdots\\ \tau_{xz}^{N-1,N}\end{Bmatrix} \quad (36)$$

where $[H]$ and $[H_o]$ collect the coefficients in (35). Inverting it, we get

$$\tau_{xz}^{i,i+1}=\sum_{j=1}^{N-1}H_{i,j}^{-1}\left[\widehat{u}(j+1)-\widehat{u}(j)\right]-[L_{i,1}]\,\phi_x^o \quad (37)$$

where the matrix $[L_{i,1}]$ is

$$[L_{i,1}] = \frac{1}{2}[H]^{-1}[H_o] \tag{38}$$

Next, calculating the difference between the interlaminar stresses in terms of the difference between the average displacements across the $N+1$ interfaces including the top and the bottom surface of the laminate, we get

$$\tau_{xz}^{i,i+1} - \tau_{xz}^{i-1,i} = \sum_{j=1}^{N-1} \left[H_{i,j}^{-1} - H_{i-1,j}^{-1} \right] [\widehat{u}(j+1) - \widehat{u}(j)] - [L_{i,1} - L_{i-1,1}]\, \phi_x^o \tag{39}$$

Since the first lamina is denoted $i = 1$, the bottom surface of the laminate is denoted with superscript "$0,1$" and since the bottom surface of the laminate is a free surface, we have $\tau_{xz}^{0,1} = 0$ and $H_{0,j} = 0$. For the top surface of the laminate, $i = N$, $\tau_{xz}^{N,N+1} = 0$ and $H_{N+1,j} = 0$ for the same reason.

5 Equilibium

Since the intralamimar stress is assumed to be linear in each lamina, its slope is constant (see Figure 5), and it can be calculated dividing (39) by the lamina thickness h_i. Therefore, the 3D equations of equilibrium reduce to 2D as follows

$$\frac{\partial \widehat{\sigma}_x^i}{\partial x} + \frac{\tau_{xz}^{i,i+1} - \tau_{xz}^{i-1,i}}{h_i} = 0 \tag{40}$$

where $\widehat{\sigma}_x$ and τ_{xz} are functions of x, and $i = 1 \ldots N$ is the lamina number. Averaging the constitutive equation (16) using (21) we obtain

$$\widehat{\sigma}_x^i = E_x^i \left(\bar{z}_i \frac{\partial \phi_x^o(x)}{\partial x} + \frac{\partial \widehat{u}_1^i(x)}{\partial x} \right) \tag{41}$$

where $\widehat{u}_1^i$ is function of x only. Substituting (39),(41), into (40) we get

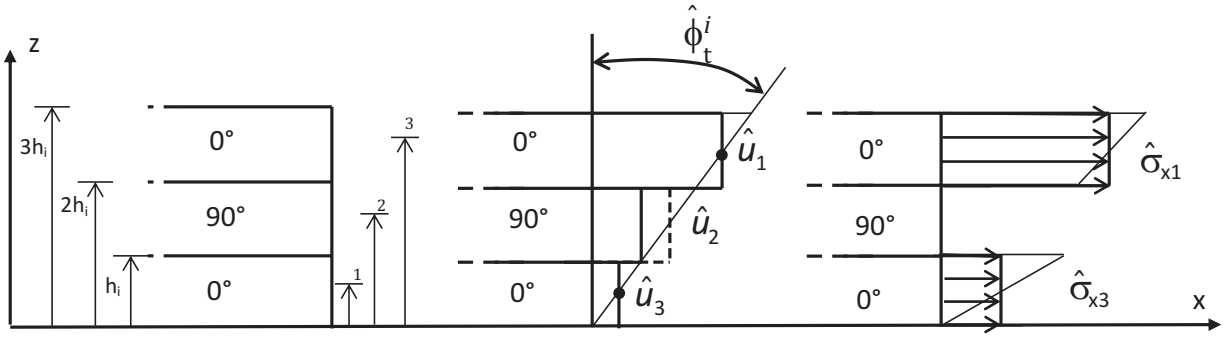

Figure 7: Averaged stresses and displacements for a $[0/90/0]_S$ laminate. Only the top half of the symmetric laminate is shown. The cracked lamina is numbered $k = 5$ with fiber orientation $\theta = 90°$.

$$E^i_x\left(\bar{z}_i\frac{\partial^2\phi^o_x(x)}{\partial x^2}+\frac{\partial^2\widehat{u}^i_1(x)}{\partial x^2}\right)-\frac{[H^{-1}_{i-1,1}-H^{-1}_{i,1}]}{h_i}\widehat{u}(1)+\frac{[H^{-1}_{i,1}-H^{-1}_{i-1,1}-H^{-1}_{i,2}+H^{-1}_{i-1,2}]}{h_i}\widehat{u}(2)$$
$$+\ldots+\frac{[H^{-1}_{i,2}-H^{-1}_{i-1,2}-H^{-1}_{i,N-1}+H^{-1}_{i-1,N-1}]}{h_i}\widehat{u}(N-1)+\frac{[H^{-1}_{i,N-1}-H^{-1}_{i-1,N-1}]}{h_i}\widehat{u}(N)$$
$$-\frac{[L_{i,1}-L_{i-1,1}]}{h_i}\phi^o_x=0 \tag{42}$$

for all $i = 1...N$ laminas.

Note that (42) is expressed in terms of the fundamental solution $\phi^o_x(x)$ (first and last terms), plus a perturbation $\widehat{u}^i_1$ (due to crack formation, see first term), plus the total displacement $\widehat{u}(i)$ of each lamina. In order to solve the problem, we need to express (42) in terms of a single dependent variable, and to express all the terms in the global coordinate system. To accomplish this, we choose the total rotation $\widehat{\phi}^i_t$ as the dependent variable, x as the independent variable, and we decompose the total displacement as follows

$$\widehat{u}^i(x)=\bar{z}_i\,\widehat{\phi}^i_t \tag{43}$$

where $\bar{z}_i$ is the location of the midsurface of lamina i and $\widehat{\phi}^i_t$ is the total rotation angle, common to all laminas for $i = 1...N$ due to compatibility of deformation between the RVE and the rest of laminate (Figure 7).

Letting $\ddot{\phi}_t = \partial^2\widehat{\phi}_t/\partial x^2$, (42) can be written as

$$\bar{z}_i[M]\{\ddot{\phi}_t^i\} + \bar{z}_i[K]\{\phi_t^i\} - [\alpha_o]\phi_x^o = 0 \tag{44}$$

where $[M]$ is the axial stiffness matrix, $[K]$ is the interlaminar stiffness matrix, and $[L_o] = (L_{i,1} - L_{i-1,1})/h_i$, and $\bar{z}_i$ is the location of the midsurface of lamina i. Equation (44) is a system N second order, ordinary differential equations with constant coefficients. As such, it admits a closed form, analytical solution, that we see to find next. To do this, the first step is to transform (44) into a so-called *standard problem*

$$\ddot{\phi}_t^i + [D]\phi_t^i = [F]\phi_x^o \tag{45}$$

where $[D] = [R]^{-1}[E]$, $[R] = \bar{z}_i[M]$, $[E] = \bar{z}_i[K]$, and $[F] = [R]^{-1}[L_o]$ for all the laminas $i = 1...N$. Next, the matrix $[D]$ can be re-written in terms of its eigenvalues $[\lambda]$ and eigenvectors $[V]$ as

$$[D] = [V][\lambda][V]^{-1} \tag{46}$$

Next, applying the change of variable

$$\{\ddot{Z}\} = [V]^{-1}\{\ddot{\phi}_t^i\} \tag{47}$$

we can *uncouple* the system of ordinary differential equations (noting that $[\lambda]$ is diagonal) as follows

$$\{\ddot{Z}_i\} + [\lambda]\{Z_i\} = [J]\phi_x^o \tag{48}$$

where $[J] = [V]^{-1}[F]$. Next, the fundamental solution ϕ_x^o can be calculated integrating (17), obtaining

$$\phi_x^o(x) = \delta_{11}\ M_x\ x \tag{49}$$

Therefore, equation (48) can be further simplified to

$$\{\ddot{Z}_i\} + [\lambda]\{Z_i\} = [J_o]x \tag{50}$$

where $[J_o] = [J]\ \delta_{11}\ M_x$. Next, note that (50) admits an exact *homogeneous* solution plus a *particular* solution, as follows

$$Z_i = r_i \exp(x\sqrt{-\lambda_i}) + s_i \exp(-x\sqrt{-\lambda_i}) + \frac{J_{oi}}{\lambda_i}x \tag{51}$$

where λ_i are the eigenvalues of $[D]$, J_{oi} are known constants for each i lamina, and r_i, s_i, are constants to be found in terms of the *boundary conditions*. The total angle rotation of the laminate can be written for each lamina as a summation, but the angle is unique for all laminas (see Figure 7), so we can drop the superscript, as follows

$$\widehat{\phi}_t = \widehat{\phi}_t^i = \sum_{j=1}^{N} V_{ij} Z_j \tag{52}$$

Taking the origin of the global coordinate system at the center of the representative volume element (RVE), as shown in Figure 1, the y-z plane is a plane of symmetry. Therefore, $\widehat{\phi}_t(\text{x=0}) = 0$, and $s_i = -r_i$, which allows us to write (51) as

$$Z_i = r_i \left(\exp(x\sqrt{-\lambda_i}) - \exp(-x\sqrt{-\lambda_i})\right) + \frac{J_{oi}}{\lambda_i}x \tag{53}$$

and furthermore, since the eigenvalues are all negative, (53) can be written as

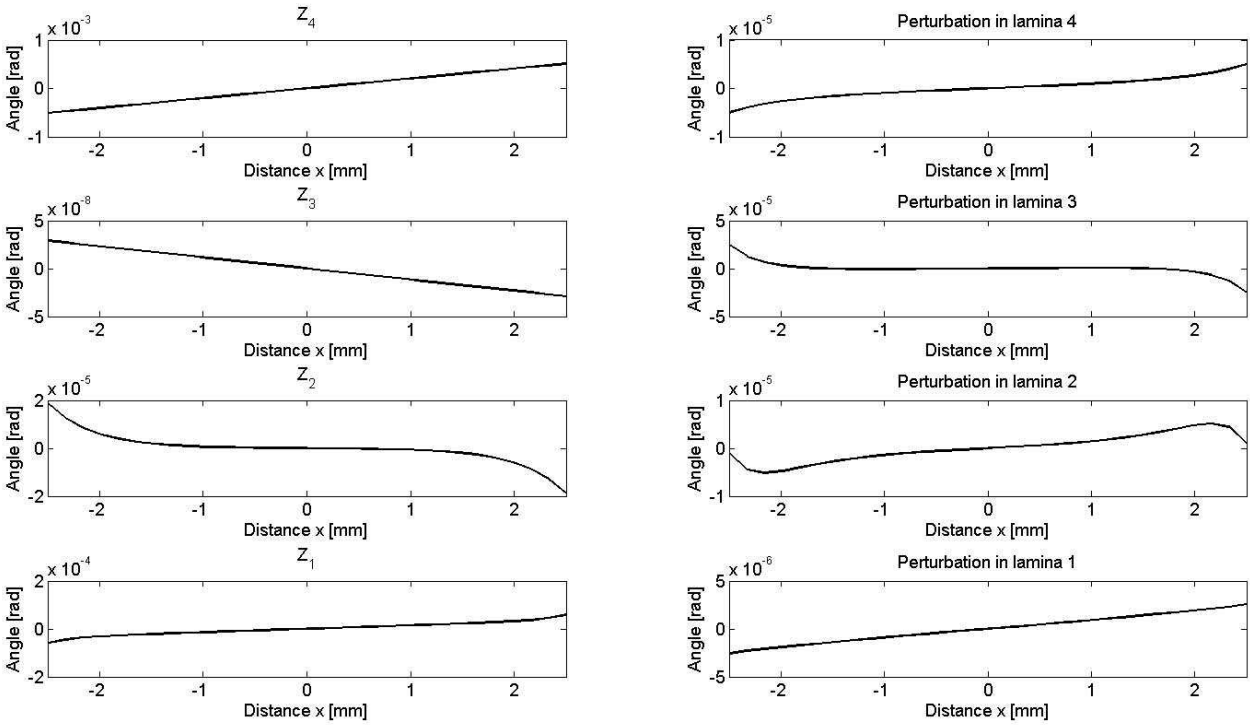

Figure 8: Left: elemental functions. Right: Deformation components. LSS: $[0_2/90_4]_S$ with $\lambda_k = 0.2\ [1/mm]$. The cracking lamina is the third one from bottom ($k = 3$).

$$Z_i = p_i \sinh(x\sqrt{-\lambda_i}) + \frac{J_{oi}}{\lambda_i}x; \quad i = 1 \dots N \tag{54}$$

where $p_i = 2r_i$.

Equation (54) implies that the total rotation angle $\widehat{\phi}_t$ in (52) is a summation of hyperbolic and linear functions, as shown on the left hand side of Figure 8. Both components are needed to describe the sum of the fundamental solution ϕ_x^0 plus the perturbations near the crack at $\pm\ell$. The fundamental solution ϕ_x^0 is described by a linear combination of terms $(J_{oi}/\lambda)x$ in (54). For a given value of x, the fundamental solution is a constant, equal to the rotation angle of FSDT, which obviously produces a linear displacement $u_x^0(z)$ as in FSDT.

For a constant applied moment M_x, the homogeneous deformation ϕ_x^o is almost linear in $-\ell < x < \ell$. To describe a linear function of x with $\sinh(x\sqrt{-\lambda_s})$, the eigenvalue λ_s must be extremely small, so that the *sinh* becomes almost linear in that range. In fact, numerical results confirm that

such eigenvalue is extremely small for every case analyzed in this work. For the example described in Fig. 8, the eigenvalue is λ_3 and the corresponding function Z_3 is virtually linear in x. Let's label the *small* eigenvalue with the subscript s. Then, $s = 3$ in Fig. 8.

A very small eigenvalue results in a very small amplitude for the *sinh*, thus a very large constant p_s is needed to recover the deformation. This pair of very small/very large eigenvalue/constant causes numerical problems. To avoid such problems, the homogeneous deformation can be approximated by a zero eigenvalue ($\lambda = 0$) and a linear function $Z_s = x$. Then, (52) is rewritten as

$$\widehat{\phi}_t = \widehat{\phi}_t^i = \sum_{j=1}^{N} (1 - \delta_{js}) V_{ij} Z_j + V_{is} B_o x \tag{55}$$

where λ_s is the almost-zero eigenvalue and B_o is part of the fundamental solution ϕ_x^0. In summary, the $s-$column of the eigenvector matrix $[V]$ is not used in the first term on the right hand side of (55) because it corresponds to an almost-zero eigenvalue; but the term canceled by $(1 - \delta_{js})$ is recovered by introducing the last term in (55), which uses the $s-$column of the eigenvector, i.e, V_{is}. Since the rest of functions Z_j, with $j \neq s$, are each a linear combination of perturbations (first term in (54)) and portions of the homogeneous deformation (second term in (54)), equation (55) the can be rewritten in terms of the curvature $\kappa_x^0 = \delta_{11}\, M_x$ obtained by FSDT (17–18), as follows

$$\widehat{\phi}_t = \sum_{j=1}^{N} (1 - \delta_{js}) V_{ij} Z_j' + \kappa_x^0\, x \tag{56}$$

where the perturbation functions Z_i' are given by the first therm in (54), i.e.,

$$Z_j^{'} = p_i \sinh(x\sqrt{-A_i}) \tag{57}$$

5.1 Boundary conditions

5.1.1 Compatible deformation on the boundary

The deformation of the boundary of the RVE must be compatible with the rest of the laminate. In this case, it means that the total rotation of all laminas, except the cracking one, must be the same

$$\widehat{\phi}_t^m(\pm\ell) = \widehat{\phi}_t^r(\pm\ell); \quad \forall\, m \neq k \tag{58}$$

where lamina r is a lamina that is not cracking, taken as reference. In the computer implementation, $r = 1$ if lamina 1 is not cracking, else $r = 2$.

5.1.2 Stress free crack surface

The cracking lamina k has cracks on the extremes of the RVE at $x = -\ell, \ell$, as shown in Figure 1. Crack surfaces are stress free, as follows

$$\int_{-1/2}^{1/2} \widehat{\sigma}_x^k(\ell)\, dy = 0 \tag{59}$$

where the integration limits represent a RVE that has unit length in the y-direction, i.e., in the fiber direction of the cracking lamina. Using (43), we get

$$E_x^k \int_{-1/2}^{1/2} \left(\bar{z}_k \frac{\partial \phi_t^k(\ell)}{\partial x} - \widehat{\alpha}_x^k \Delta T \right) dy = 0 \tag{60}$$

which simplifies to

$$\dot{\phi}_t^k(\ell) = \dot{\phi}_t^k(-\ell) = \frac{\widehat{\alpha}_x^k \Delta T}{\bar{z}_k} \tag{61}$$

5.1.3 External load

The applied bending load M_x, if any, is applied to the boundary of all the laminas except the cracked one because the later has a free surface on the boundary. Therefore, the load equilibrium on the boundary of the RVE excludes the cracked lamina, as follows

$$\sum_{i=1}^{N}(1-\delta_{ik})\int_{-1/2}^{1/2}\int_{h_i}\widehat{\sigma}_x^i(\ell)\,z dz dy = M_x \tag{62}$$

where $h=\sum_{i=1}^{N}h_i$ is the thickness of the laminate, k is the cracking lamina, δ is the Kronecker symbol, and M_x is the bending load applied to the laminate. Using (43),

$$\sum_{i=1}^{N}(1-\delta_{ik})E_x^i\int_{-1/2}^{1/2}\int_{h_i}\left(\bar{z}_k\frac{\partial\phi_t^i(\ell)}{\partial x}-\widehat{\alpha}_x^k\Delta T\right)z dz dy = M_x \tag{63}$$

where

$$\int_{h_i}z dz = \frac{z^2}{2}\bigg|_{z^{i-1,i}}^{z^{i,i+1}} = h_i\bar{z}_i \tag{64}$$

which simplifies to

$$\sum_{i=1}^{N}(1-\delta_{ik})E_x^i h_i\bar{z}_i^2\dot{\phi}_t^i = M_x+\sum_{i=1}^{N}(1-\delta_{ik})E_x^i h_i\bar{z}_i\widehat{\alpha}_x^i\Delta T \tag{65}$$

Note that away from the crack, the cracked lamina still supports load, which is transfered from the uncracked to the cracked laminas by intralaminar shear in the vicinity of the crack.

6 Reduced Laminate Stiffness

The boundary conditions described in the previous section allows us to determine the constants p_i in (57) for $i\neq s$, that is $N-1$ values; plus B_o to obtain κ_x^0 from (17) yields N equations for N

unknowns, which are the average displacements $\widehat{u}_i$ in N layers. To do this, one substitutes (55) into the boundary conditions (58), (61), and (65). In the context of this study, the load is defined by a pair (bending moment, temperature), i.e., $(M_x, \Delta T)$.

Applying $M_x = 1, \Delta T = 0$, allows us to calculate the degraded modulus of the laminate E_x^b as a function of crack density λ_k. When a unit bending load $M_x = 1$ is applied, the homogenized laminate curvature is obtained by averaging the curvature from (56) as follows

$$\widehat{\kappa}_x^0 = \frac{1}{2\ell}\int_{-\ell}^{\ell} \frac{\partial \widehat{\phi}_t(x)}{\partial x} dx = \frac{\widehat{\phi}_t(\ell)}{\ell} \tag{66}$$

It follows that to calculate the engineering modulus, the inverse of δ_{11} is needed

$$\delta_{11}^{-1} = \frac{M_x}{\widehat{\kappa_x^0}} \quad ; \quad \text{for } M_x = 1, \Delta T = 0 \tag{67}$$

Finally, the bending modulus of the laminate is

$$E_x^b = \frac{12}{h_t^3\ \delta_{11}^{-1}} = \frac{12\,\ell}{h_t^3\ \widehat{\phi}_t(\ell)} \tag{68}$$

which is determined by the average total rotation at $x = \ell$, calculated with (66) and (56).

7 Results and discussion

Two materials have been selected for this section, Fiberity/HyE-9082A [28,29] and Avimid-K/IM6 [37]. The material properties are tabulated in [38].

7.1 Results

The results are presented in Figures 9, 10, 11 for two materials and several laminates. In the plots, the "laminate moduli by CLT" is the flexural modulus of the undamaged laminate, and the "Laminate reduced stiffness" is the flexural modulus $E_x^b(\lambda)$ calculated with (68). The drop is

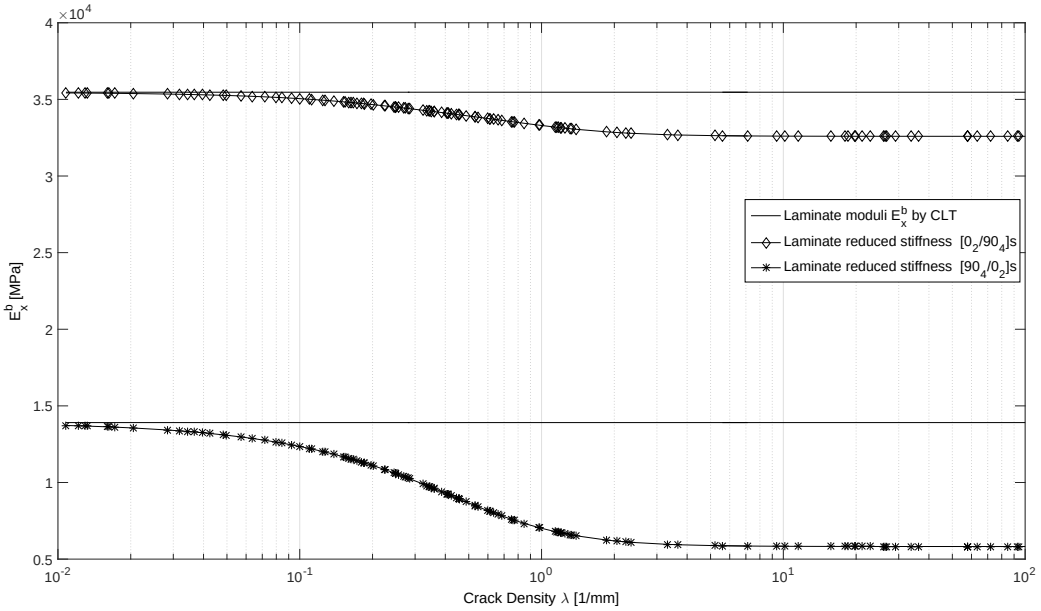

Figure 9: Prediction of laminate flexural modulus E_x^b vs. crack density λ for $[0_2/90_4]_S$ and $[90_4/0_2]_S$ Fiberite/HyE-9082A.

physically caused by the cracks and numerically captured by the $N-1$ perturbation terms of the solution (56).

In Figure 9, the modulus drops 7.98% (from 35.42 to 32.59 MPa) for $[0_2/90_4]_S$ and 57.58% (from 13.72 to 5.82 MPa) for $[90_4/0_2]_S$. The later laminate starts with lower flexural modulus because the transverse laminas are on the outside, and looses a larger percentage of its stiffness because the cracking lamina is on the outside as well.

In Figure 10, the modulus drops 10.08% (from 32.22 to 28.97 MPa) for $[\pm 15/90_4]_S$, 11.99% (from 24.37 to 20.23 MPa) for $[\pm 30/90_4]_S$, and 21.77% (from 19.11 to 14.95 MPa) for $[\pm 40/90_4]_S$. The later laminate starts with lower flexural modulus because the outside laminas at ± 40 are less stiff than for the other two laminates, and looses a larger percentage of its stiffness because the cracking lamina represents a larger % of the total stiffness of the laminate.

In Figure 11, the modulus drops 4.37% (from 82.01 to 78.42 MPa) for $[0/90_3]_S$ and 54.46% (from 11.76 to 5.35 MPa) for $[90_3/0]_S$. The later laminate starts with lower flexural modulus because the transverse laminas are on the outside, and looses a larger percentage of its stiffness because the cracking lamina is on the outside as well.

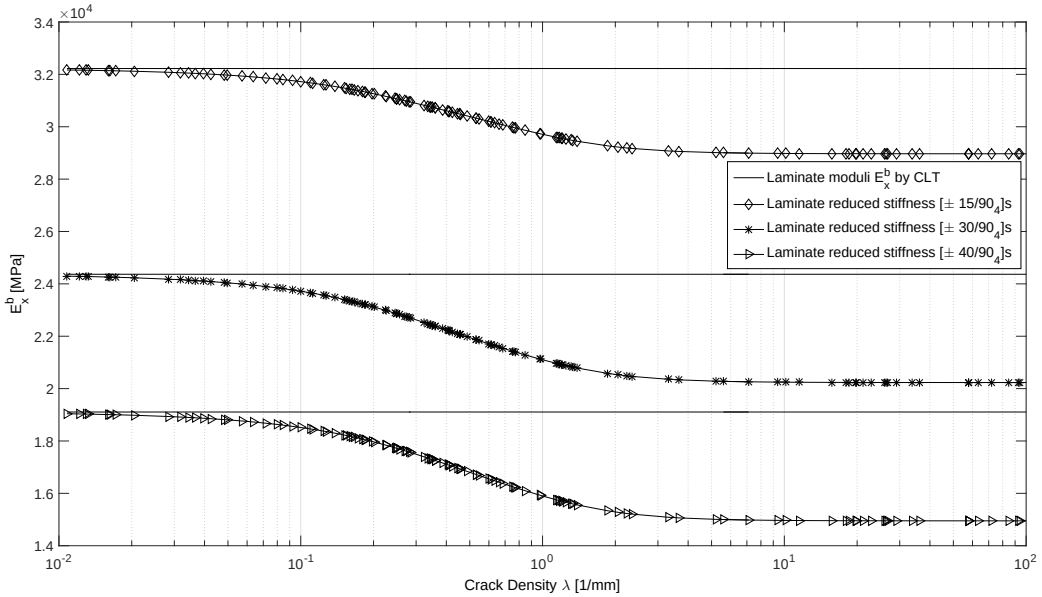

Figure 10: Prediction of laminate flexural modulus E_x^b vs. crack density λ for $[\pm\theta/90_4]_S$ Fiberite/HyE-9082A with $\theta = 15, 30, 40$.

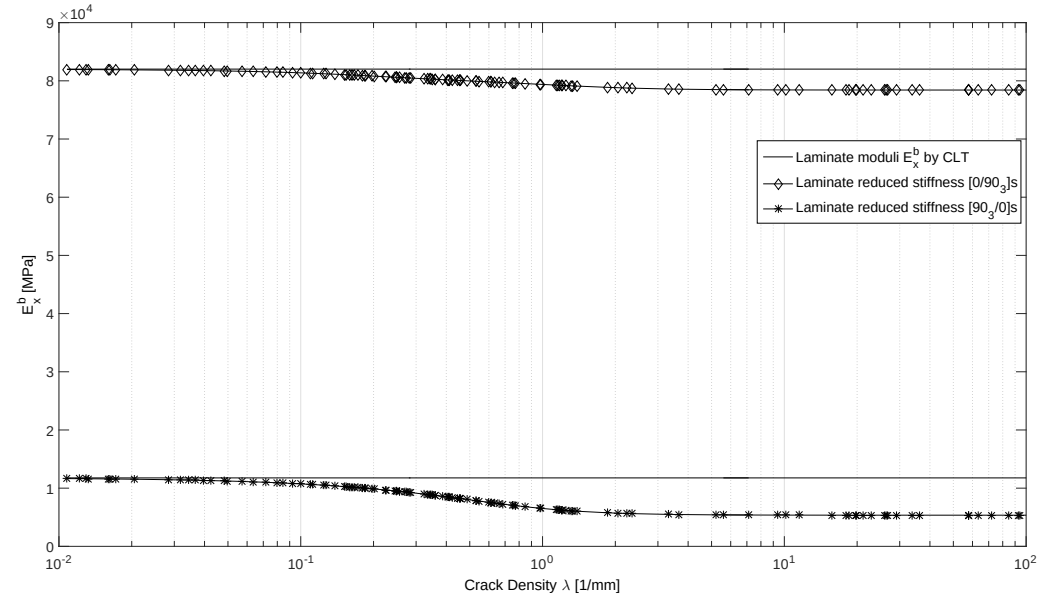

Figure 11: Prediction of laminate flexural modulus E_x^b vs. crack density λ for $[0/90_3]_S$ and $[90_3/0]_S$ Avimid-K/IM6.

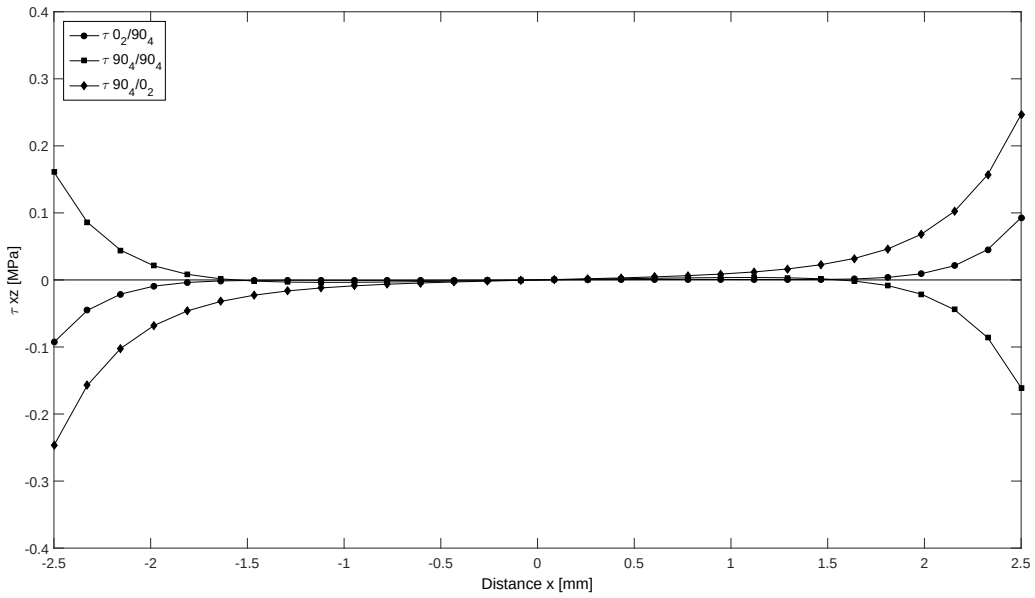

Figure 12: Intralaminar stress $\tau_{xz}(x)$ at the interfaces (see legend) of a $[0_2/90_4]_S$ Fiberite/HyE-9082A laminate subjected to bending $M_x = 1$ N mm, with crack density $\lambda_k = 0.25$ on the tensile side of the 90_4 layer.

7.2 Intralaminar stress fields

Intralaminar stress are necessary near the crack to transfer the load between the loaded laminas (denoted by subscript m) and the cracked lamina (denoted by subscript k). The intralaminar stress vanishes far away from the crack, once all of the load has been redistributed in the laminate.

Calculated intralaminar stress $\tau_{xz}(x)$ between two cracks located at $x = \pm\ell$ are shown in Figure 12 for the interfaces 0/90 in a $[0_2/90_4]_S$ laminate and in Figure 13 for the four interfaces in a $[0/\pm 15/90_2]_S$ Fiberite/HyE-9082A. In the legend, the interfaces are denoted by the pair of angles of the adjacent laminas. The intralaminar stress τ_{xz} is higher at the crack locations (located at $\pm\ell$) and the interface $90_4/0_2$ above the midsurface of the laminate has the maximum values because it is located next to the cracked 90_4 lamina on the tensile side of the laminate.

Calculated intralaminar stress through the thickness $\tau_{xz}(z)$ at the crack surface located at $x = \ell$ is shown in Figure 14 for the $[0_2/90_4]_S$ Fiberite/HyE-9082A laminate. Recall that $\tau_{xz} = 0$ at the top and bottom surface because they are a free surfaces. The cracking thickness is $4t_k + e_b$, where $t_k = 0.144$ mm is the ply thickness and $e_b = 0.0103$ mm is the position of the neutral axis due to cracking, calculated by (13).

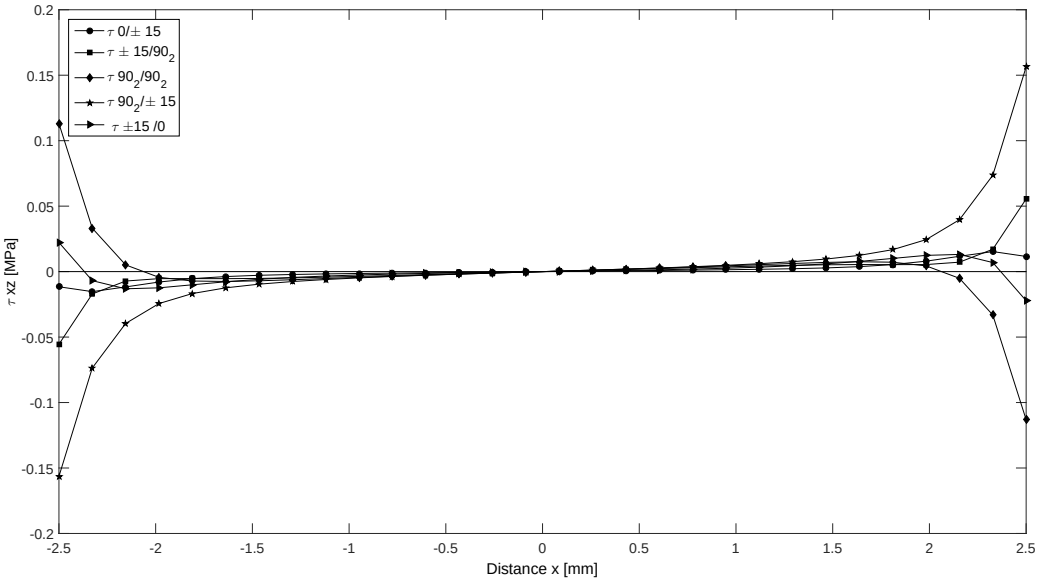

Figure 13: Intralaminar stress $\tau_{xz}(x)$ at the interfaces (see legend) of a $[0/\pm 15/90_2]_S$ Fiberite/HyE-9082A laminate subjected to bending $M_x = 1$ N mm, with crack density $\lambda_k = 0.25$ on the tensile side of the 90_4 layer.

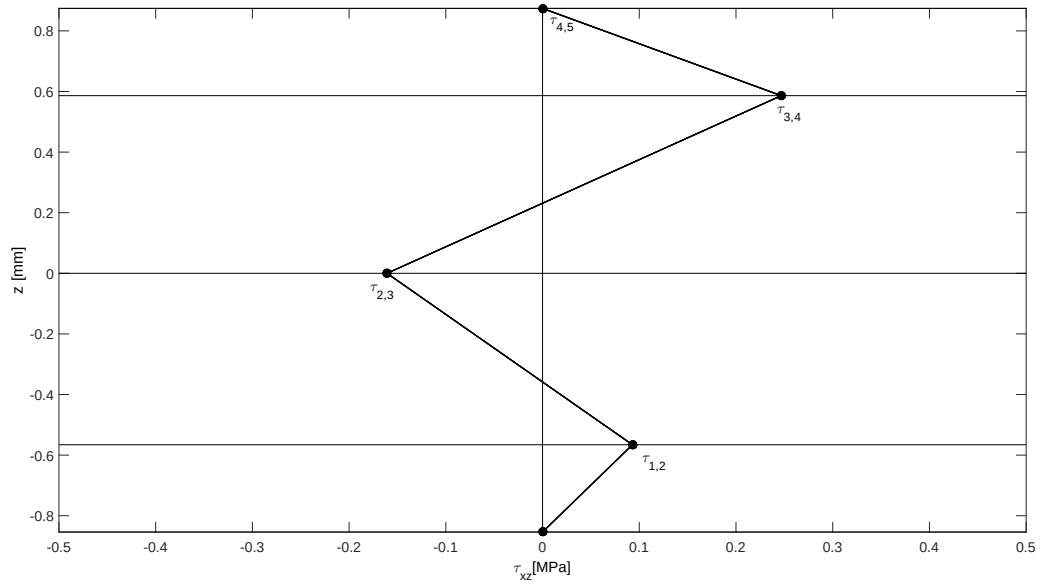

Figure 14: Intralaminar stress $\tau_{xz}(\ell)$ through the thickness of a $[0_2/90_4]_S$ Fiberite/HyE-9082A laminate subjected to bending $M_x = 1$ N mm, with crack density $\lambda_k = 0.25$ on the tensile side of the 90_4 layer.

Note that the approximation can be refined by modeling individual laminas, even if they are adjacent and have the same orientation, instead of lumping them together into a single, thicker, equivalent lamina. Furthermore, it is possible to refine the model by sub-dividing laminas into a number n of sub-laminas. This cannot be done with the cracking lamina because the crack spans the entire thickness. To show the effect of model refinement, intralaminar stress through the thickness $\tau_{xz}(z)$ at the crack surface located at $x = \ell$ for the $[0_2/90_4]_S$ Fiberite/HyE-9082A laminate are shown in Figure 14 for $n = 1$, Figure 15 for $n = 2$, Figure 16 for $n = 4$, and Figure 17 for $n = 8$, where n is the number of subdivisions in each of the 0_2 laminas.

It can be seen that the maximum value at the 90/0 interface (labeled $\tau_{3,4}$ in Fig. 14) increases slightly with the number of sub-laminas. This means that the assumption of linear intralaminar stress is not exact, but a very good approximation. Furthermore, the maximum value of intralaminar stress converges as the number of sub-laminas (in a piece-wise representation on intralaminar stress) increases from 1 to 8. The convergence plot is shown in Figure 18.

Also, it can be seen, particularly in Figure 17, that the maximum interlaminar stress occurs at the interface between the cracking and uncracking laminas. Also, it is worth noticing that all formulations in the literature use linear distribution of intralaminar stress, not only in the adjacent lamina but over an entire, equivalent sub-laminate that often encompasses all of the intact (non damaging) laminas on either side (top and bottom) of the cracking lamina, e.g., [3, 39].

7.3 Displacement components

The elementary functions Z_i that result from the exact solution to the problem are shown in Figure 8 (left) for the $[0_2/90_4]$ laminate. It can be seen that Z_4 is linear, resulting in a linear *component* of angle rotation $\widehat{\phi}_1^i = V_{i4}Z_4$ for all laminas i, with constant angle ϕ_x^o; where $\widehat{\phi}_t^i = \phi_x^o + \widehat{\phi}_1^i$. The remaining components are perturbations that appear in the exact solution to produce the intralaminar stress that redistributes the load between cracked and intact laminas.

The displacement perturbations in each lamina $\widehat{u}(i) - \bar{z}_i\phi_x^o$ are shown in Figure 8 (right). In the literature, the magnitude of the ineffective length δ (the shear lag) is often assumed because it is very difficult to calculate. However, the proposed methodology allows for calculation of the ineffective length using the exact solution for the perturbations. The distance δ for which the perturbations decrease (typically a 10% of their maximum value [40–42]), are hereby calculated

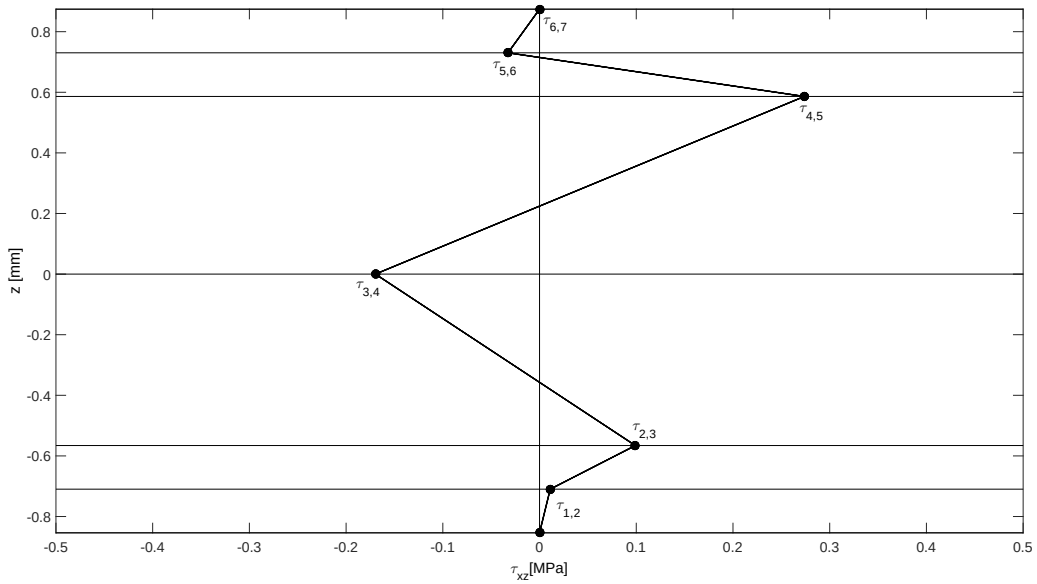

Figure 15: Intralaminar stress $\tau_{xz}(\ell)$ through the thickness of a $[0_2/90_4]_S$ under bending $M_x = 1$ N mm, with crack density $\lambda_k = 0.25$ on the tensile side of the 90_4 layer. The 0° lamina divided into *two* sub-laminas.

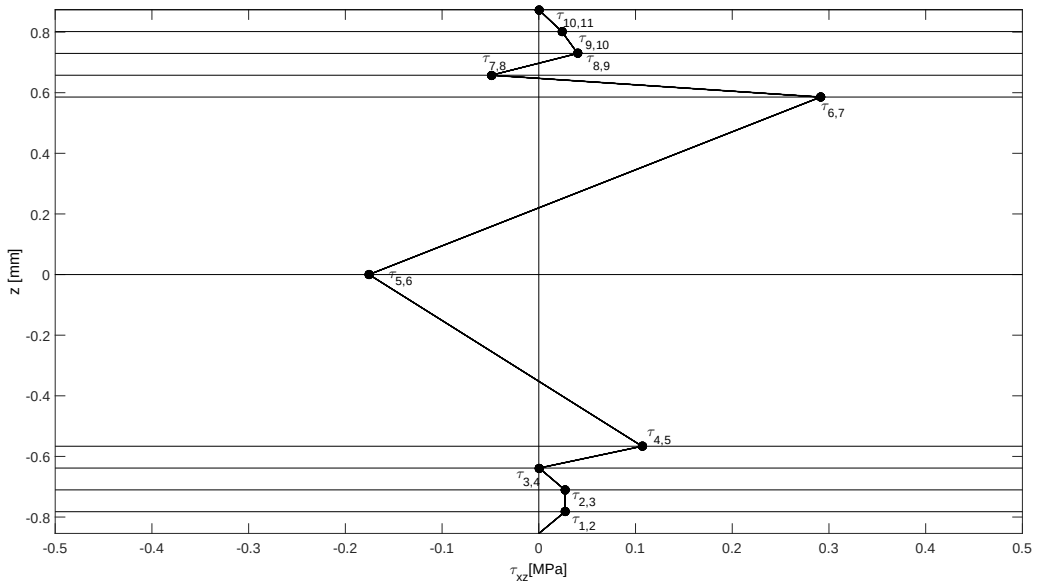

Figure 16: Intralaminar stress $\tau_{xz}(\ell)$ through the thickness of a $[0_2/90_4]_S$ under bending $M_x = 1$ N mm, with crack density $\lambda_k = 0.25$ on the tensile side of the 90_4 layer. The 0° lamina divided into *four* sub-laminas.

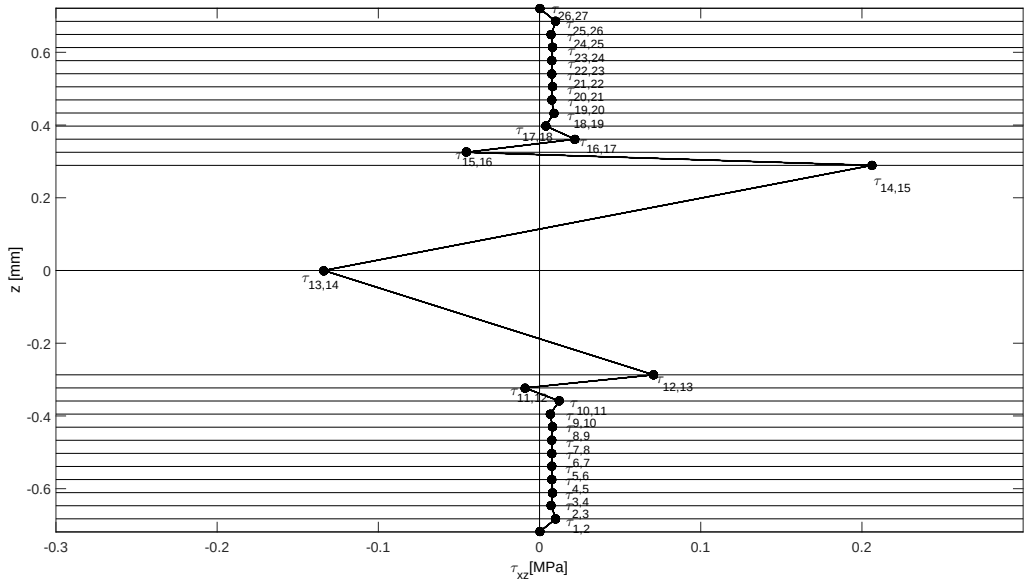

Figure 17: Intralaminar stress $\tau_{xz}(\ell)$ through the thickness of a $[0_2/90_4]_S$ under bending $M_x = 1$ N mm, with crack density $\lambda_k = 0.25$ on the tensile side of the 90_4 layer. The 0° lamina divided into *eight* sub-laminas.

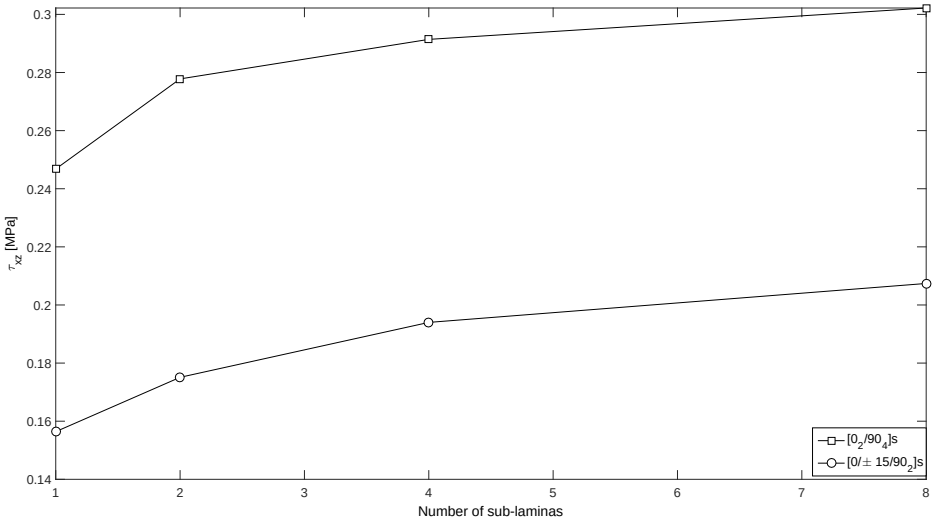

Figure 18: Maximum intralaminar stress $\tau_{xz}(\ell)$ as a function of the number of sub-laminas in the 0 and ±15 laminas. The maxima occur at the 90/0 and 90/±15 interfaces, thus they are *interlaminar* stresses.

Laminate	*Interface*	δ [mm]	τ_{xz} $[MPa]$
$[0/\pm 15/90_2]_S$	$0/\pm 15$	1.41	0.015
	$\pm 15/90_2$	0.501	0.055
	$90_2/90_2$	0.3067	0.113
	$90_2/\pm 15$	0.6971	**0.156**
	$\pm 15/0$	**1.647**	0.022
$[0_2/90_4]_S$	$0_2/90_4$	0.517	0.0929
	$90_4/90_4$	0.586	0.161
	$90_4/0_2$	**1.011**	**0.247**

Table 1: Ineffective length δ calculated from the results reported in Figures 12–13 for $M_x = 1$ N mm.

from the results reported in Figures 12–13, and reported in Table 1.

Note that the largest interlaminar stress occurs at the interfaces between the cracked and uncracked laminas on the tensile side (interface $90_2/\pm 15$ for the $[0/\pm 15/90_2]_S$ laminate and interface $90_4/0_2$ for the $[0_2/90_4]_S$ laminate). Qualitatively, these trends are to be expected. However, the present methodology provides *quantitative* values, which so far could be obtained only through numerical methods such as FEA. Furthermore, note that the longer ineffective length may occur at interfaces between laminas that are not cracking, e.g., at the $\pm 15/0$ interface of the $[0/\pm 15/90_2]_S$ laminate, although neither the ± 15 or the 0 laminas are cracked.

To illustrate the capability of the formulation to analyze non-symmetric laminates, results are presented in Figure 19, compared to the undamaged CLT solution for the same laminates. The largest relative reduction of flexural stiffness occurs for the $[0_2/90_4]$ because the top lamina (90_4) is in tension and thus the laminate looses most of its flexural stiffness when transverse matrix cracks develop. Similarly, the $[0_3/90_4]$ also looses most of its flexural stiffness, even though the 0_3 lamina is 50% thicker then the 0_2 layer. Thus, in both laminates discussed so far, $[0_2/90_4]$ and $[0_3/90_4]$, the undamaged 90_4 lamina serves to position the stiff longitudinal laminas away from the neutral axis, and most of the flexural stiffness of the laminate is due to that effect. In comparison, the $[90_4/0_3/90]$ laminate, has less initial stiffness because of the position of the longitudinal lamina near the neutral axis, and it looses less of that stiffness when the relatively thin top lamina develops significant damage, as seen in the Figure.

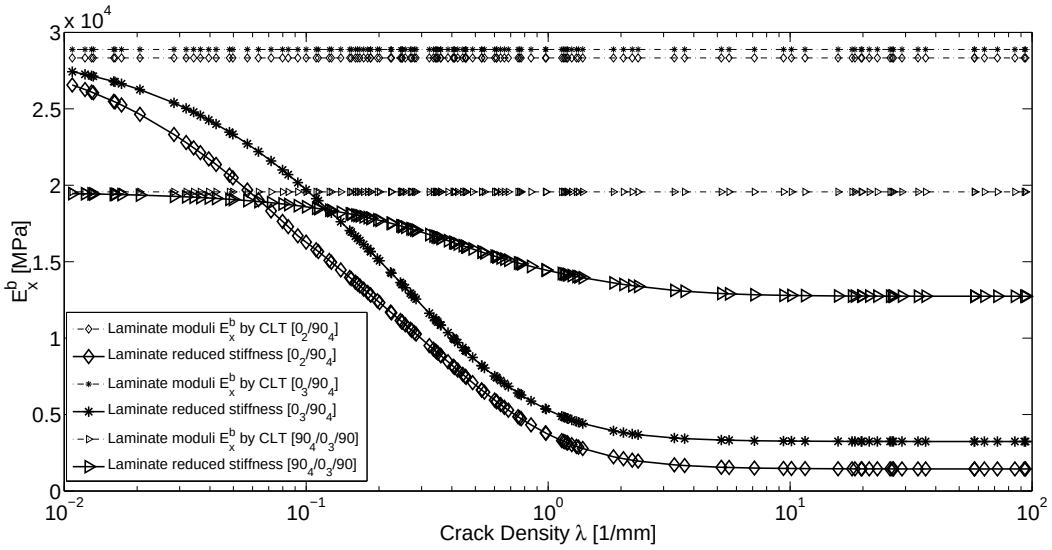

Figure 19: Flexural modulus vs. crack density for non-symmetric laminates.

7.4 Condition number

The condition number for an eigenvalues problem is defined as ratio between the maximum and minimum eigenvalue. Ordering the eigenvalues by descending value, the condition number of the full matrix $[V]$ in (52) is $C_n = \lambda_1/\lambda_n \gg 1$, with very large values that are unfavorable for numerical computation. This happens because $\lambda_n \approx 0$. On the contrary, the condition number of the reduced-rank matrix $(1-\delta_{is})V_{ij}$ in (56) is $C_{n-1} = \lambda_1/\lambda_{n-1} \sim 10^1$, which is favorable for numerical computation. Using (56) instead of (52) leads us to obtain a condition number C_{n-1} of order one. A comparison of condition number between the original eigenvalue problem (with a rank N matrix) and the new one (with a rank $N-1$ matrix), is shown in Table 2.

8 Conclusions

A closed form, analytical solution for a laminated beam with transverse cracks subjected to bending is presented. The solution provides an analytical, yet approximate solution for the average displacement of each lamina as well as the overall rotation of the laminate, the later being a correction of the (undamaged) FSDT solution to account for damage. From the rotation and displacements, both axial and intralaminar strains and stresses can be resolved analytically. The analysis is restricted to balanced but not necessarily symmetric laminates subjected to bending. The solution includes

Material	*Laminate*	C_n	C_{n-1}	λ_1	λ_{n-1}	λ_n
I	$[0_2/90_4]_S$	$3.267e+16$	54.830	-26.373	-0.4806	-8.074e-16
I	$[90_4/0_2]_S$	$132e+16$	42.175	-52.382	-1.242	-3.988e-16
I	$[\pm 15/90_4]_S$	$9.290e+16$	54.192	-28.9931	-0.535	-3.121e-16
I	$[\pm 30/90_4]_S$	$1.691e+16$	53.740	-39.391	-0.733	-2.335e-15
I	$[\pm 40/90_4]_S$	$1.947e+16$	54.775	-51.544	-0.941	-2.647e-15
II	$[0/90_3]_S$	$4.342e+16$	54.034	-18.966	-0.351	-4.368e-16
II	$[90_3/0]_S$	$5.893e+16$	3.746	-10.187	-2.719	-1.729e-15

I: IM6(Carbon)/Avimid-K II: Fiberite(Glass)/HyE-9082A

Table 2: Condition number C and eigenvalues λ.

calculation of the reduced stiffness of the laminate as a function of crack density, as well as intralaminar stresses, interlaminar stresses, and ineffective length. Calculation of intralaminar/interlaminar stresses can be refined by subdividing the intact laminas into sublaminates. *Interlaminar* stresses can be reported for the entire length of the interfaces between cracks. *Intralaminar* stress can be reported for the entire thickness at any location between cracks. The results show the expected trends, such as larger percentage reduction of flexural stiffness when the cracking laminas are away from the midsurface of the specimens. Besides expected trends, it provides quantitative information that is useful for the design of experiments. For example, it is clear that some laminate configurations with an expected stiffness loss of only 4% would not be useful to elucidate the effects of damage in an experimental setting because the change in stiffness would be of the order of magnitude of the precision of the instrumentation. Other LSS using the same material and lamina thicknesses could provide 50% or more resolution. Also, the analytical solution can be used as a benchmark for numerical methods.

References

[1] M. M. Moure, S. Sanchez-Saez, E. Barbero, E. J. Barbero, Analysis of damage localization in composite laminates using a discrete damage model, Composites Part B 66 (2014) 224–232.

[2] G. J. Dvorak, N. Laws, M. Hejazi, Analysis of progressive matrix cracking in composite laminates i. thermoelastic properties of a ply with cracks, Journal of Composite Materials 19 (3) (1985) 216–234.

[3] S. C. Tan, R. J. Nuismer, A theory for progressive matrix cracking in composite laminates, Journal of Composite Materials 23 (1989) 1029–1047.

[4] T. Yokozeki, T. Aoki, Stress analysis of symmetric laminates with obliquely-crossed matrix cracks, Advanced Composite Materials 13 (2) (2004) 121–40.

[5] L. N. McCartney, Energy-based prediction of progressive ply cracking and strength of general symmetric laminates using an homogenisation, Method, Composites Part A 36 (2005) 119–128.

[6] L. N. McCartney, Energy-based prediction of failure in general symmetric laminates, Engineering Fracture Mechanics 72 (2005) 909–930.

[7] E. J. Barbero, L. DeVivo, Constitutive model for elastic damage in fiber-reinforced pmc laminae, International Journal of Damage Mechanics 10 (1) (2001) 73–93.

[8] P. Ladevèze, O. Allix, J. Deü, D. Lévêque, A mesomodel for localisation and damage computation in laminates, Computer Methods in Applied Mechanics and Engineering 183(1-2) (2000) 105–122.

[9] F. Rastellini, S. Oller, O. Salomón, E. Oñate, Composite materials non-linear modelling for long fibre-reinforced laminates: Continuum basis, computational aspects and validations, Computers and Structures 86(9) (2008) 879–896.

[10] X. Martinez, F. Rastellini, S. Oller, F. Flores, E. O. nate, Computationally optimized formulation for the simulation of composite materials and delamination failures, Composites Part B: Engineering 42(2) (2011) 134–144.

[11] E. J. Barbero, F. A. Cosso, R. Roman, T. L. Weadon, Determination of material parameters for Abaqus progressive damage analysis of E-Glass Epoxy laminates, Composites Part B:Engineering 46 (2013) 211–220.

[12] P. Lonetti, R. Zinno, F. Greco, E. J. Barbero, Interlaminar damage model for polymer matrix composites, Journal of Composite Materials 37 (16) (2003) 1485–1504.

[13] E. J. Barbero, F. Greco, P. Lonetti, Continuum damage-healing mechanics with application to self-healing composites, International Journal of Damage Mechanics 14 (1) (2005) 51–81.

[14] Simulia, Abaqus Theory Manual, §32.5.6, Version 6.12 (2012).

[15] F. Greco, L. Leonetti, P. Lonetti, A novel approach based on ale and delamination fracture mechanics for multilayered composite beams, Composites Part B: Engineering 78 (2015) 447–458.

[16] Z. Hashin, Analysis of cracked laminates: a variational approach, Mechanics of Materials 4 (121) (1985) 121–136.

[17] J. Zhang, J. Fan, C. Soutis, Analysis of multiple matrix cracking in $[\pm\theta/90_n]_s$ composite laminates, part I, inplane stiffness properties, Composites 23 (5) (1992) 291–304.

[18] E. Adolfsson, P. Gudmundson, Thermoelastic properties in combined bending and extension of thin composite laminates with transverse matrix cracks, International Journal of Solids and Structures 34 (16) (1997) 2035–2060.

[19] E. Adolfsson, P. Gudmundson, Matrix crack initiation and progression in composite laminates subjected to bending and extension, International Journal of Solids and Structures 36 (21) (1999) 3131–3169.

[20] A. Adumitroaie, E. J. Barbero, Intralaminar damage model for laminates subjected to membrane and flexural deformations, Mechanics of Advanced Materials and Structures 22 (9) (2015) 705–716. doi:10.1080/15376494.2013.796541.

[21] P. A. Smith, S. L. Ogin, On transverse matrix cracking in cross-ply laminates loaded in simple bending, Composites Part A: Applied Science and Manufacturing 30 (8) (1999) 1003–1008.

[22] P. A. Smith, S. L. Ogin, Characterization and modelling of matrix cracking in a (0/90)2s GFRP laminate loaded in flexure, Proceedings of the Royal Society of London, Series A (Mathematical, Physical and Engineering Sciences) 456 (2003) (2000) 2755–70.

[23] S. Li, S. R. Reid, P. D. Soden, Modelling the damage due to transverse matrix cracking in fiber-reinforced laminates, in: Proc. 2nd Int. Conf. on Nonlinear Mechanics (ICNP-2), Peking University Press, 1993, pp. 320–323.

[24] S. Li, S. R. Reid, P. D. Soden, A finite strip analysis of cracked laminates, Mechanics of Materials 18 (4) (1994) 289–311.

[25] S. Li, S. R. Reid, P. D. Soden, A continuum damage model for transverse matrix cracking in laminated fibre-reinforced composites, Philosophical Transactions of the Royal Society London, Series A (Mathematical, Physical and Engineering Sciences) 356 (1746) (1998) 2379–412.

[26] A. High Smith, Stiffness reduction mechanisms in composite laminates, in: Damage in Composite Materials, ASTM, 1982, p. 15.

[27] S. G. Lim, C. S. Hong, Effect of transverse cracks on the thermomechanical properties of cross-ply laminated composites, Composites Science and Technology 34 (2) (1989) 34–2.

[28] J. Varna, R. Joffe, N. Akshantala, R. Talreja, Damage in composite laminates with off-axis plies, Composites Science and Technology 59 (1999) 2139–2147.

[29] J. Varna, R. Joffe, R. Talreja, A synergistic damage mechanics analysis of transverse cracking in $[\pm\theta/90_4]_s$ laminates, Composites Science and Technology 61 (2001) 657–665.

[30] J. Nairn, Matrix microcracking in composites, in: R. Talreja, J. A. E. Manson (Eds.), Polymer Matrix Composites, Vol. 2 of Comprehensive Composite Materials, Elsevier, Amsterdam, 2000, pp. 403–432.

[31] J. Nairn, S. Hu, Matrix microcracking, in: R. Talreja (Ed.), Damage Mechanics of Composites Materials, Elsevier, 2004, pp. 187–243.

[32] S. Kobayashi, N. Takeda, Experimental characterization of microscopic damage behavior in carbon/bismaleimide composite–effects of temperature and laminate configuration, Composites Part A 33 (11) (2002) 1529–1538.

[33] T. Yokozeki, T. Aoki, T. Ishikawa, Consecutive matrix cracking in contiguous plies of composite laminates, International Journal of Solids and Structures 42 (9-10) (2005) 2785–2802.

[34] E. J. Barbero, Introduction to Composite Materials Design, 2nd Edition, CRC Press, Philadelphia, PA, 2011.

[35] A. M. Abad Blazquez, M. Herraez Matesanz, C. Navarro Ugena, , E. J. Barbero, Acoustic emission characterization of intralaminar damage in composite laminates, in: MATCOMP XIII, Algeciars, Spain, 2013, pp. 33–38.

[36] E. J. Barbero, J. Cabrera Barbero, C. Navarro Ugena, Analytical solution for plane stress/strain deformation of laminates with matrix cracks, Composite Structures.

[37] S. Liu, J. A. Nairn, Formation and propagation of matrix microcracks in cross-ply laminates, J Reinf Plas Compos (1992) 158–178.

[38] E. J. Barbero, F. A. Cosso, Benchmark solution for degradation of elastic properties due to transverse matrix cracking in laminated composites, Composite Structures 98 (2013) 242–252.

[39] R. J. Nuismer, S. C. Tan, Constitutive relations of a cracked composite lamina, Journal of Composite Materials 22 (1988) 306–321.

[40] B. W. Rosen, Tensile failure of fibrous composites, AIAA Journal 2 (11) (1964) 1985–1991.

[41] E. J. Barbero, K. W. Kelly, Predicting high temperature ultimate strength of continuous fiber metal matrix composites, Journal of Composite Materials 27 (12) (1993) 1214–1235.

[42] K. W. Kelly, E. J. Barbero, Effect of fiber damage on the longitudinal creep of a cfmmc, International Journal of Solids and Structures 30 (24) (1993) 3417–3429.